Backscatter in the Rational LES Model

Traian Iliescu [a]

[a] *Mathematics and Computer Science Division, Argonne National Laboratory, Argonne, IL 60439, U.S.A.*

Paul Fischer [b]

[b] *Mathematics and Computer Science Division, Argonne National Laboratory, Argonne, IL 60439, U.S.A.*

Abstract

This paper presents a comparison for the backscatter (the inverse transfer of energy from small to large scales) in the rational and the gradient large eddy simulation (LES) models. We applied both LES models in the numerical simulation of turbulent channel flows at $Re_\tau = 180$ and $Re_\tau = 395$. The rational LES model yielded improved results and was more stable numerically.

Key words: large-eddy simulation, turbulence, backscatter.

1 Introduction

Large eddy simulation (LES) aims at capturing the large, energy-containing scales in turbulent flow, while modeling the interaction between the large and small scales. Most of the commonly used models assume that the essential function of the unresolved (modeled) scales is to remove energy from the large scales and dissipate it through the action of viscous forces. While, on average, energy is transferred from the large to the small scales ("forward scatter"), it has been recognized that the inverse transfer of energy from small to large scales ("backscatter") may be quite significant and should be included in the LES model.

Email addresses: `iliescu@mcs.anl.gov` (Traian Iliescu), `fischer@mcs.anl.gov` (Paul Fischer).

The Smagorinsky model (14) is one of the most popular LES models. This classical eddy-viscosity model is, however, purely dissipative and cannot predict backscatter. To include backscatter, the Smagorinsky model is usually used in the dynamical framework. This approach may, however, lead to numerical instabilities.

A few LES models introduce backscatter in a *natural* way. This paper presents a numerical investigation of backscatter in two such LES models (the rational and the gradient LES models) applied to the numerical simulation of turbulent channel flows at $Re_\tau = 180$ and $Re_\tau = 395$.

2 Mathematical and Numerical Setting

The usual LES starts by convolving the Navier-Stokes equations (NSEs) with a spatial filter g_δ. Assuming that differentiation and convolution commute, the filtered NSEs read as follows:

$$\overline{\mathbf{u}}_t + \nabla \cdot (\overline{\mathbf{u}\mathbf{u}}) - Re^{-1} \Delta \overline{\mathbf{u}} + \nabla \overline{p} = \overline{\mathbf{f}}, \tag{1}$$

where δ is the filter width and $\overline{\mathbf{u}} = g_\delta * \mathbf{u}$ is the variable of interest. The filtered NSEs (1) do not form a closed system, and a considerable research effort in LES has been directed at modeling the stress

$$\tau = \overline{\mathbf{u}\mathbf{u}} - \overline{\mathbf{u}}\,\overline{\mathbf{u}}. \tag{2}$$

As mentioned by Carati et al. (2), this stress consists of a filtered-scale stress tensor, mainly due to filtering, and a subgrid-scale (SGS) stress tensor, mainly due to discretization. One way of approximating the filtered-scale stress tensor is by using a Taylor series expansion in the wave number space to represent the unknown full velocity in terms of the filtered velocity. This approach was first used in (11), and later in (3). The resulting model, called the gradient, nonlinear, or tensor-diffusivity model, was used in numerous studies (11), (3), (2), (15):

$$\tau = \overline{\mathbf{u}\mathbf{u}} - \overline{\mathbf{u}}\,\overline{\mathbf{u}} \approx \frac{\delta^2}{2\gamma} \nabla\overline{\mathbf{u}}\nabla\overline{\mathbf{u}}, \quad \text{where} \quad (\nabla\overline{\mathbf{u}}\nabla\overline{\mathbf{u}})_{i,j} = \sum_{l=1}^{d} \frac{\partial \overline{\mathbf{u}}_i}{\partial \mathbf{x}_l} \frac{\partial \overline{\mathbf{u}}_j}{\partial \mathbf{x}_l}. \tag{3}$$

Noticing that the approximation by Taylor series of $\widehat{g_\delta}$ actually *increases* the high wave number components, Galdi and Layton (6) developed a new LES model based on a rational ((0,1) Padé) approximation of $\widehat{g_\delta}$, which preserves the decay of the high wave number components.

The resulting LES model, called the rational LES (RLES) model, reads as follows:

$$\tau = \left[\left(-\frac{\delta^2}{4\gamma}\Delta + I \right)^{-1} \left(\frac{\delta^2}{2\gamma} \nabla\overline{\mathbf{u}}\nabla\overline{\mathbf{u}} \right) \right]. \tag{4}$$

The inverse operator in (4) acts as a smoothing operator and represents the approximation of the convolution by the Gaussian filter in the stress tensor τ in (2).

The mathematical analysis associated with the RLES model (4) was presented in (1). The first steps in the numerical analysis and validation of the RLES model (4) were made in (9) and (10), respectively.

In (8), we compared the RLES model (4) with the gradient model (3) in 3D channel flow simulations at Reynolds numbers based on the wall shear velocity $Re_\tau = 180$ and $Re_\tau = 395$. In our numerical simulations we used a spectral element code.

For this paper, we collected statistics for the SGS dissipation, the forward and backscatter for the RLES model (4), and the gradient model (3) in channel flow simulations at $Re_\tau = 180$ and $Re_\tau = 395$. We started with field files corresponding to LES simulations in (8), which had already reached a statistically steady state. We then integrated the flow further in time and collected statistics for the above three quantities, which were averaged over time and homogeneous directions (streamwise and spanwise.) All three statistics were normalized by u_τ^3, where u_τ is the computed wall-shear velocity, which was found to be within $1\% - 2\%$ of the nominal value.

The model subgrid-scale dissipation was computed as

$$\epsilon_{SGS} := \tau_{ij}\, \overline{S}_{ij}, \tag{5}$$

where $\overline{S}_{ij} = \frac{1}{2}\left(\frac{\partial \overline{\mathbf{u}}_i}{\partial \mathbf{x}_j} + \frac{\partial \overline{\mathbf{u}}_j}{\partial \mathbf{x}_i} \right)$ represents the large-scale strain-rate tensor.

The model subgrid-scale dissipation ϵ_{SGS} represents the energy transfer between the resolved and the unresolved (subfilter-scale) scales. If ϵ_{SGS} is negative, energy is transferred from large scales to small scales (forward scatter); if ϵ_{SGS} is positive, energy is transferred from small scales to large scales (backscatter). We denote the forward scatter by $\epsilon_+ = \frac{1}{2}(\epsilon_{SGS} + |\epsilon_{SGS}|)$ and the backscatter by $\epsilon_- = \frac{1}{2}(\epsilon_{SGS} - |\epsilon_{SGS}|)$.

3 Numerical Results

In the $Re_\tau = 180$ case, the model subgrid-scale dissipation ϵ_{SGS} in Figure 1 shows the correct behavior for the RLES model (4): the forward scatter is dominant throughout the channel, with a peak near the wall. This behavior can be noticed in the DNS results in (4) (Figure 8a, p. 2159.)

The correct ϵ_{SGS} is quite challenging to capture in LES: The velocity estimation model in (4) (Figure 8a, p. 2159) underpredicts the correct peak value of ϵ_{SGS}. The variational multiscale approach in (7) underpredicts significantly the correct peak value for ϵ_{SGS} (Figure 14, p. 1791.) The ϵ_{SGS} corresponding to the RLES model in Figure 1 performs better than both previous methods; the RLES model actually performs similarly to the classical eddy-viscosity models (the Smagorinsky model in (4) and the Smagorinsky model with Van Driest damping in (7).) This is quite remarkable for a *non* eddy-viscosity model such as the RLES model, which introduces significant amount of backscatter.

The gradient model (3) has an incorrect behavior: It starts with a huge amount of backscatter near the wall and then reaches the peak value of forward scatter away from the correct location (4).

The forward and backscatter in Figure 1 illustrate the smoothing character of the inverse filtering in the RLES model (4): the "spikes" corresponding to the gradient model are damped in the RLES model. This process has a positive effect on the numerical stability of the RLES model. The huge amount of forward and backscatter introduced by the gradient model in the near-wall region is responsible for the unstable behavior in wall-bounded flow simulations (15).

For both LES models, the backscatter and the forward scatter contributions to the SGS dissipation were comparable, and each was much larger than the total SGS dissipation. This behavior was also noticed in (12).

In the $Re_\tau = 395$ case, the SGS dissipation corresponding to the RLES model (4) in Figure 2 is much less than that for the gradient model (3); the latter seems exaggerated for this Reynolds number. The forward and backscatter for the RLES model are, however, larger than those for the gradient model. This fact does not contradict the observation about the SGS dissipation, since ϵ_{SGS} is the sum of the forward and backscatter. We also need to keep in mind that, although both LES models are started from the same initial conditions, the corresponding flows are evolved in time *differently*. Thus, in the numerical simulations, the SFS stress tensor τ in the RLES model is *not* simply the inverse operator in (4) applied to the SFS stress tensor τ in the gradient model.

As in the $Re_\tau = 180$ case, for both LES models the backscatter and the forward scatter contributions were comparable, and each was much larger than the total SGS dissipation (12).

We note that the RLES model is more stable numerically than the gradient model. Actually, the gradient model (3) blew up a few hundred time steps after we stopped collecting statistics. This unstable behavior has been observed in similar calculations in (15). There, as a remedy ad hoc wall-damping functions were used.

We also note the unphysical spikes corresponding to the gradient model (3) in all three quantities monitored: ϵ_{SGS}, ϵ_-, and ϵ_+. These spikes are located exactly at the interfaces between adjacent spectral elements. This behavior is natural, since the SGS tensor τ for the gradient model (3) contains products of gradients of the computed velocity (see (3)). The RLES model, on the other hand, smoothes out these spikes through its inverse operator; this smoothing makes the RLES model more stable numerically. Further investigation of these issues is necessary.

4 Conclusions

We applied the RLES model (4) and the gradient model (3) in the numerical simulation of turbulent channel flows at $Re_\tau = 180$ and $Re_\tau = 395$. We gathered statistics for the model SGS dissipation, the forward scatter, and the backscatter. In the $Re_\tau = 180$ case, the RLES model (4) yielded much improved results, closer to the DNS results in (4). The gradient model introduced an unphysical amount of backscatter near the wall, which made the computations more unstable. In the $Re_\tau = 395$ case, the RLES model's SGS dissipation was closer to a realistic value. The SGS dissipation for the gradient model seemed unrealistically high. The amount of forward and backscatter was, however, higher for the RLES model. Despite this, the gradient model (3) was more unstable numerically, as reported in (15). This issue deserves further investigation.

Both the RLES and the gradient models introduce backscatter in a *natural* way. The gradient model is unstable in numerical simulations. On the contrary, the RLES model, through the action of its smoothing filter, makes the computations much more stable; it can run for thousands of time steps without additional numerical stabilization procedures.

Acknowledgments. This work was supported in part by the Mathematical, Information, and Computational Sciences Division subprogram of the Office of Advanced Scientific Computing Research, U.S. Dept. of Energy, under Contract W-31-109-Eng-38.

References

[1] Berselli LC, Galdi GP, Iliescu T, Layton WJ. Mathematical analysis for the rational large eddy simulation model. Math. Models and Methods in App. Sci. 2002; 12(8):1-22.

[2] Carati D, Winckelmans GS, Jeanmart H. On the modeling of the subgrid-scale and filtered-scale stress tensors in large-eddy simulation. J. Fluid Mech. 2001; 441:119-138.

[3] Clark RA, Ferziger JH, Reynolds WC. Evaluation of subgrid scale models using an accurately simulated turbulent flow, J. Fluid Mech. 1979; 91:1-16.

[4] Domaradzki JA, Saiki EM. A subgrid-scale model based on the estimation of unresolved scales of turbulence. Phys. Fluids 1997; 9(7):2148-2164.

[5] Fischer P, Iliescu T. A 3D channel flow simulation at $Re_\tau = 180$ using a rational LES model. In Liu C, Sakell L, Beutner T, editor. Proceedings of Third AFOSR International Conference on DNS/LES. Arlington, USA: Greyden Press, 2001. p. 283-290.

[6] Galdi GP, Layton WJ. Approximating the larger eddies in fluid motion II: a model for space filtered flow. Math. Models and Methods in App. Sci. 2000; 10:343-350.

[7] Hughes TJR, Oberai AA, Mazzei L. Large eddy simulation of turbulent channel flows by the variational multiscale method. Phys. Fluids, 2001; 13(6):1784-1799.

[8] Iliescu T, Fischer P. Large eddy simulation of turbulent channel flows by the rational LES model. Preprint ANL/MCS-P938-0302 2002.

[9] Iliescu T, John V, Layton WJ. Convergence of finite element approximation of large eddy motion. Num. Meth. Part. Diff. Eq., accepted 2002.

[10] Iliescu T, John V, Layton WJ, Matthies G, Tobiska L. A numerical study of a class of LES models. Int. J. Comput. Fluid Dyn., accepted 2002.

[11] Leonard A. Energy cascade in large eddy simulations of turbulent fluid flows. Adv. in Geophysics 1974; 18A:237.

[12] Piomelli U, Cabot WC, Moin P, Lee S. Subgrid-scale backscatter inturbulent and transitional flow. Phys. Fluids A 1991; 3(7):1766-1771.

[13] Sagaut P. Large Eddy Simulation for Incompressible Flows. Berlin: Springer Verlag, 2001.

[14] Smagorinsky J. General circulation experiments with the primitive equation: I the basic experiment. Mon. Wea. Rev. 1963; 91:99-164.

[15] Winckelmans GS, Wray AA, Vasilyev OV, Jeanmart H. Explicit-filtering large-eddy simulations using the tensor-diffusivity model supplemented by a dynamic Smagorinsky term. Phys. Fluids 2001; 13(5), 1385-1403.

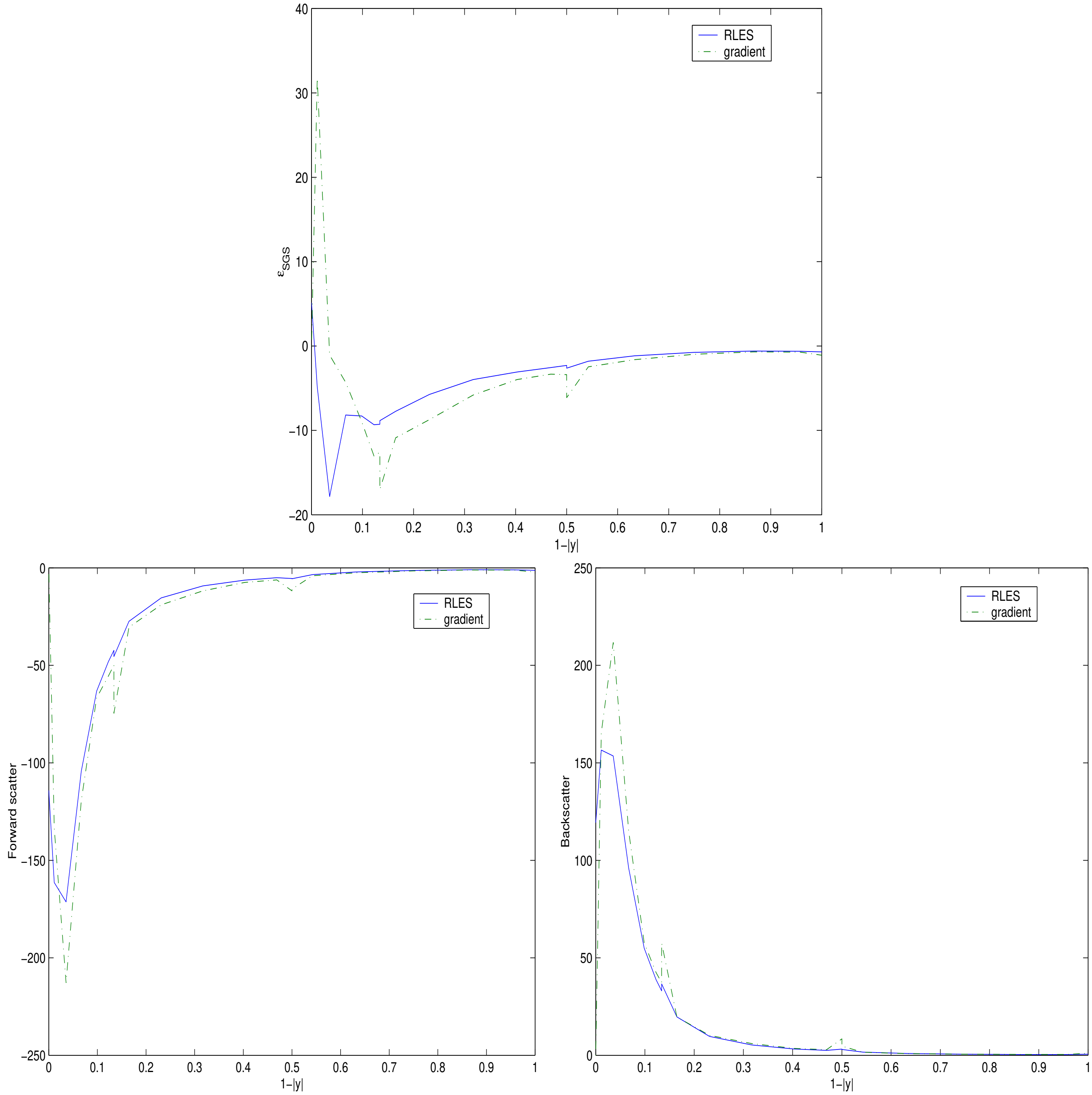

Fig. 1. $Re_\tau = 180$, the RLES model (4) and the gradient model (3): SGS dissipation (top); forward scatter (bottom, left); backscatter (bottom, right).

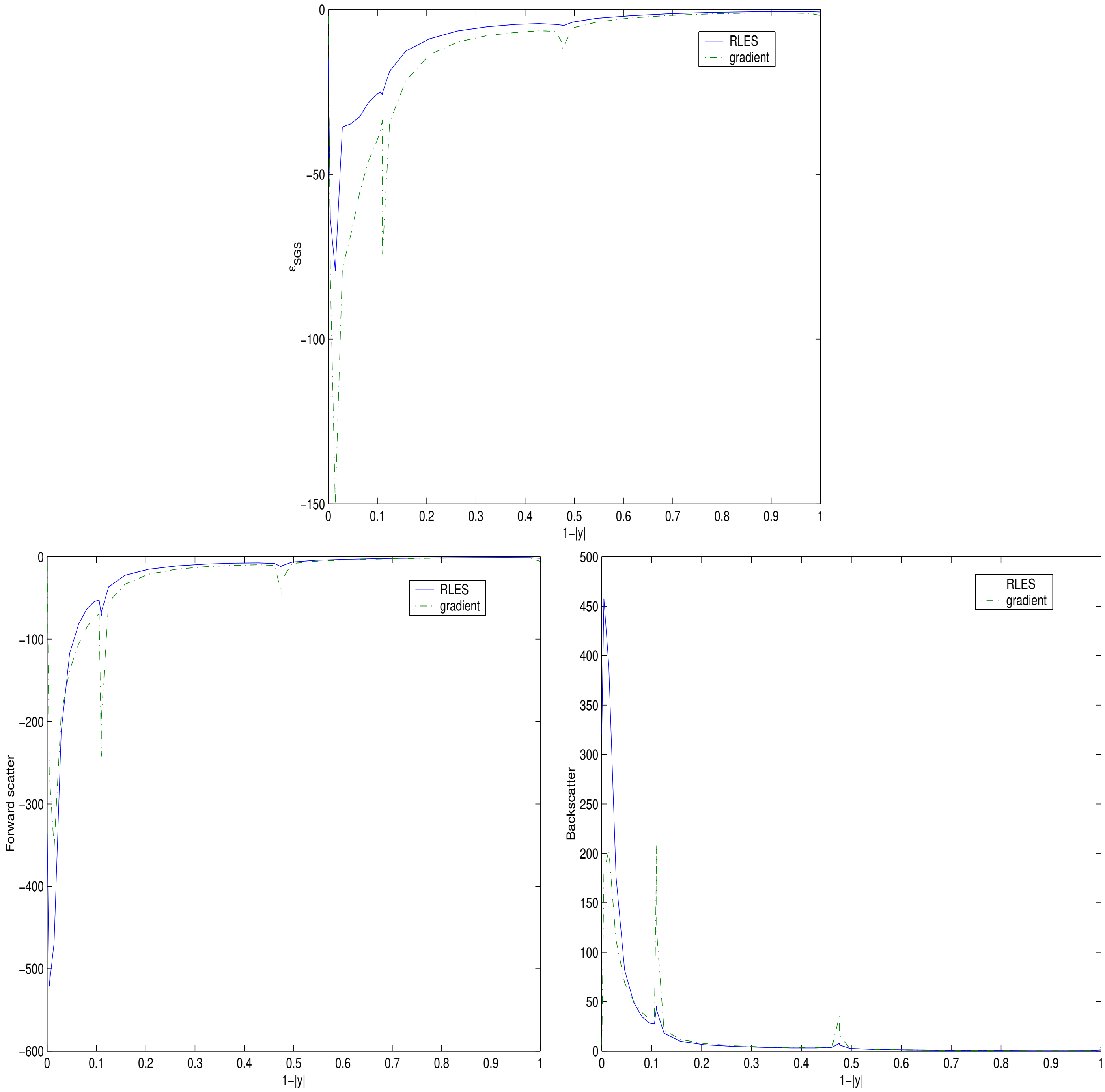

Fig. 2. $Re_\tau = 395$, the RLES model (4) and the gradient model (3): SGS dissipation (top); forward scatter (bottom, left); backscatter (bottom, right).